Indian Journal of Chemistry
Vol. 56A, April 2017, pp. 365-372

# Graphene oxide-supported gold nanocomposites for highly sensitive sandwich immunosensor for α-fetoprotein detection

Pengjun Li[a], Juanhua Lai[b] & Ping Qiu[a,]*

[a]Department of Chemistry, Nanchang University, Nanchang 330031, China

Email: pingqiu@ncu.edu.cn

[b]Jiangxi medical device testing center, Nanchang 330047, China

*Received 18 September 2016; revised and accepted 14 March 2017*

A graphene oxide-Au NPs sensor platform combined with a multiple-enzyme labeled detection antibody-carbon sphere bioconjugate has been used as the basis for an ultrasensitive electrochemical immunosensor to detect the cancer biomarker, α-fetoprotein (AFP). Greatly enhanced sensitivity has been achieved by using the bioconjugates featuring horseradish peroxidase (HRP) and Ab2 linked to carbon nanospheres (Ab2-HRP-Au-PDA-carbon sphere) at a high ratio of HRP/Ab2. After a sandwich immunoreaction, the Ab2-HRP-Au-PDA-carbon sphere captured onto the electrode surface produces an amplified electrocatalytic response due to the reduction of enzymatically oxidized thionine in the presence of hydrogen peroxide. The increase of response current is proportional to the AFP concentration in the range of 0.01-20 ng/mL, with the detection limit of 3 pg/mL. This amplification strategy is a promising platform for detection of other proteins and clinical applications.

**Keywords:** Nanocomposites, Immunosensors, Gold nanoparticles, Sandwich immunosensors, Graphene oxide, α-Fetoprotein

Immunoassays based on specific antigen-antibody recognition for analytical purposes have been an attractive subjected for clinical diagnosis[1,2] environmental analysis[3], and the food industry[4]. α-fetoprotein(AFP), an oncofetal glycoprotein with a molecular mass of about 68 kDa[5], is well-known as a tumor marker. In healthy human serum, the average concentration of AFP is typically below 25 ng/mL, and an elevated AFP concentration in adult plasma may be an early indication of some cancerous diseases including hepatocellular cancer, yolk sac cancer, liver metastasis from gastric cancer, testicular cancer, and nasopharyngeal cancer[6]. Thus, it is necessary to detect AFP for clinical diagnosis. Several methods and strategies such as fluorometry atomic studies[7], absorption spectrometry[8], and enzyme-linked immunoassay (ELISAs)[9] have been reported for the determination of AFP. Electrochemical immunoassays seem to be excellent candidates for the rapid and inexpensive diagnosis of genetic diseases and for the detection of pathogenic biological species of clinical interest, due to their advantages such as simple pretreatment procedure, fast analytical time, precise and sensitive current measurements, and inexpensive and miniaturizable instrumentation[10]. Recently, numerous immunological methods for determining the concentration of AFP by electrochemical imunoassays have been reported[11,12]. In the development of electrochemical immunosensing strategies, the stability or activity of the immobilized biocomponents and signal amplification of the immunoconjugates are two key factors[13]. Attempts have been reported in the literature to improve the stability or activity of the immobilized biocomponents by using various novel materials such as organic-inorganic composite materials[14], carbon nanotubes[15], and other nanomaterials[16].

Carbon nanomaterials have attracted considerable attention in electrochemical biosensors because of their extraordinary physical properties and remarkable conductivities[17]. While CNTs have been widely used as labeling particles in immunoassays with excellent sensitivity, problems that need to be overcome include nanotube heterogeneity and purity. Recently, porous carbon nanospheres (CNSs) have also displayed unique advantages owing to the tunability of particle size and shape as well as the resident porosity that promotes diffusion of guest molecules through interconnected micropores[18]. A "green" synthetic approach has been developed that involves

the transformation of sugars into homogeneous and stable colloidal CNSs, which are hydrophilic[19,20]. Such surface-functionalized CNSs and structures are potentially beneficial for labeling.

For gold electrodes, the electrocatalytic properties strongly depend on their microstructure and surface chemistry. Recently, graphene has emerged as an interesting material because of its unusual electronic properties and large accessible surface area[21,22]. Biocompatible graphene sheets as a sensor platform not only present an abundant domain for bimolecular binding, but also exhibit fast electron-transfer kinetics and further signal amplification in electrochemical detection[23,24]. For example, a novel electrode system using reduced graphene oxide as a biosensing platform has been proposed. Graphene sheets are reported to show favorable electrochemical activity to several electroactive compounds[25]. In addition, graphene electrodes exhibit a superior biosensing performance over single-walled carbon nanotubes toward dopamine detection in the presence of common interfering agents, such as ascorbic acid and serotonin[26].

Herein, we report an electrochemical immunosensor for sensitive detection of AFP based on a dual amplification mechanism resulting from multienzyme-antibody functionalized CNSs and Au NPs functionalized graphene sheets as the sensor platform. The synthesized colloidal CNSs from glucose under hydrothermal treatment were employed as a carrier for HRP-secondary antibody (HRP-Ab2) immobilization. Greatly enhanced sensitivity was achieved by using the bioconjugates featuring horseradish peroxidase (HRP) and Ab2 linked to carbon nanospheres (Ab2-HRP-Au-PDA-carbon sphere) at a high ratio of HRP/Ab2. After a sandwich immunoreaction, the Ab2-HRP-Au-PDA-CNSs captured onto the electrode surface produced an amplified electrocatalytic response by the reduction of enzymatically oxidized thionine in the presence of hydrogen peroxide. The increase of response current was proportional to the AFP concentration in the range of 0.01-20 ng/mL with the detection limit of 3 pg/mL. The proposed immunosensor shows potential applications in clinical screening of cancer biomarkers and point of-care diagnostics.

## Materials and Methods

Graphite flake (99.8%, 325 mesh) and DA hydrochloride (99%, F. wt. 189.64) was purchased from Alfa Aesar Co, (USA). AFP and anti-AFP were purchased from Biocell Co, (Zhengzhou, China). Bovine serum albumin (BSA), HRP, gold chloride ($HAuCl_4$), and sodium citrate were obtained from Sigma Chemicals. (St. Louis, USA). All other reagents were commercially available. Phosphate buffer solution (0.1 *M*) of analytical grade (PBS, pH 7.4) was used as supporting electrolyte. All solutions were prepared with doubly distilled water.

Scanning electron microscopy (SEM) images were obtained on a Quanta 200 scanning electron microscope (FEI, USA). UV-vis absorption spectra were recorded with a UV-2450 spectrophotometer (Shimadzu). Electrochemical experiments were carried out on a PGSTAT30/FRA2 system (Autolab, The Netherlands). A three-electrode system was used with a saturated calomel electrode (SCE) as the reference electrode, a platinum wire as the auxiliary electrode, and the modified AuE as the working electrode.

### Preparation of GO-Au NPs

Au NPs were synthesized according to the as-reported method[27]. Briefly, 100 mL of 1 m*M* $HAuCl_4$ was brought to reflux while stirring and then 10 mL of 38.8 m*M* trisodium citrate solution was added quickly, which resulted in a color change of the solution from pale yellow to deep red. After the color change, the solution was refluxed for an additional 15 min. The final concentration of Au NPs was fixed to 1 m*M* by evaporating excess water.

The GO was prepared from graphite flake by Hummers' method[28]. Briefly, 0.5 g of graphite, 0.5 g of $NaNO_3$ and 23 mL of $H_2SO_4$ were stirred together in an ice bath. Next, 3 g of $KMnO_4$ was gradually added under stirring, keeping the mixture below 20 °C. Subsequently, the solution was transferred to a 35±5 °C water bath and stirred for about 1 h, forming a thick paste. Next, 40 mL of ultrapure water was added. And the temperature was increased to 90±5 °C, and stirred for 0.5 h. Finally, 100 mL of ultrapure water was added, followed by the slow addition of 3 mL of $H_2O_2$ (30%). It was observed that the color of the mixture changed from dark brown to yellow and there was no gas being produced. The warm solution was then filtered and washed three times with 5% aqueous HCl to remove metal ions and then washed with ultrapure water to remove the acid. The filter cake was dispersed in ultrapure water, and the obtained brown dispersion was then subjected to 5 min of centrifugation at 3000 rpm to remove any

unexfoliated graphite oxide. Exfoliation was obtained after 2 h of ultrasonic treatment.

The preparation procedure of the GO-Au NPs hybrid is showed in Scheme 1. The GO were first functionalized with PDDA by the following procedure. A 3 mL portion of 1 mg/mL GO was dispersed in 12 mL of aqueous solution containing 0.625 *M* potassium chloride and 1.25 mg/mL PDDA. After being mixed well, the mixture was sonicated for 3 h to give a homogeneous black dispersion. Excess PDDA was removed by centrifugation, and the composite was rinsed with water twice. Finally, the PDDA/GO was redispersed in 3 mL of water. A 200 µL portion of 1 mg/mL PDDA/GO was added to 4 mL of Au NPs solution under stirring. Then, the mixture was sonicated for 2 min before standing overnight. Finally, the precipitate was collected by centrifugation and washed several times. The as-prepared GO-Au NPs mixture was redispersed in 1 mL of water.

**Preparation of Ab2-HRP-Au-PDA-carbon sphere conjugate**

Carbon sphere was synthesized from glucose in closed systems under hydrothermal conditions and characterized by electron imaging studies (SEM)[29]. Briefly, 8 g of glucose was dissolved in water (30 mL). After being mixed well, the mixture was sonicated for 0.5 h to form a clear solution, which was placed in a 40 mL teflon-sealed autoclave and maintained at 160 °C for 7 h. The puce products were isolated by centrifugation, cleaned by three cycles of centrifugation/washing/redispersion in water and in alcohol, and oven-dried at 80 °C for more than 4 h.

For synthesis of Ab2-HRP-Au-PDA-carbon sphere conjugate, HRP and Ab2 were attached to carbon sphere with a reaction mixture of 300/1 HRP/Ab2 molar ratio (Scheme 2). Briefly, 500 µL of 60 m*M* (excess) DA, 0.25 mg HRP and 8 µg Ab2 were added to 1.0 mL PBS containing 0.5 mg $mL^{-1}$ carbon sphere under vigorous stirring at 4 °C. Then, 300 µL of 2% $HAuCl_4$ was added dropwise to the mixture and the reaction mixture was stirred for 20 min to allow for completion of the reaction to form Ab2-HRP-Au-PDA-carbon sphere conjugate. After that, the reaction mixture was washed with PBS and centrifuged at 13000 rpm for 5 min three times, and the supernatant was discarded. The resulting mixture was redispersed in 1.0 mL of pH 7.4 PBS containing 1% BSA and stored at 4 °C when not used. The Ab2-HRP-Au-PDA-carbon sphere conjugate is stable and can keep enzyme activity for at least one month.

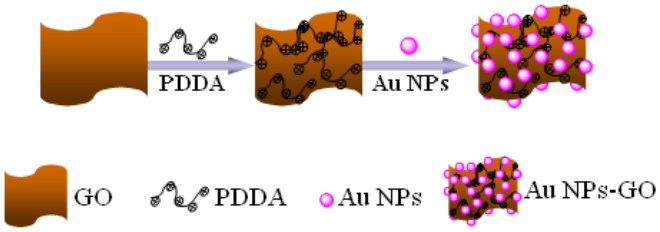


Preparation of GO-Au NPs composites

**Scheme 1**

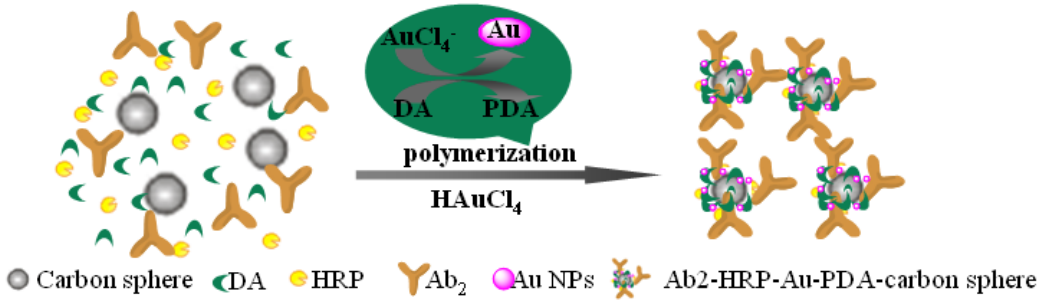


Preparation of Ab2- HRP–Au-PDA-carbon sphere conjugate

**Scheme 2**

**Fabrication of the immunosensor**

The gold electrode (AuE, 2-mm diameter) was carefully polished by 1.0, 0.3, and 0.05 μm alumina slurry, respectively, with thorough rinsing with doubly distilled water between each polishing step. The electrode was ultrasonically cleaned with 1:1 nitric acid, ethanol, and doubly distilled water, and then allowed to dry under $N_2$. Then, a 5 μL of GO-Au NPs Hybrid was cast on a pretreated Au electrode and dried at room temperature. The AuE/GO-Au NPs was immersed in 0.5 mL phosphate buffer solution (pH 7.4) with Ab1(0.50 mg/mL) solution at 4 °C for 6 h. The antibody-embedded glod electrode (denoted as AuE/GO-Au NPs/ Ab1) was soaked in 1% BSA solution for 1 h at 37.5 °C to block the non-specific sites (denoted as AuE/GO-Au NPs/ Ab1/BSA). Then AuE/GO-Au NPs/ Ab1/BSA was rinsed in doubly distilled water to remove the redundant amount of BSA. The resulting electrode was stored in the phosphate buffer solution (pH 7.4) at 4 °C until further use.

**Immunoassay procedure for detection of AFP**

A sandwich immunoassay was used for determination of AFP. The immunosensor, AuE/GO-Au NPs/ Ab1/BSA, was incubated with 0.50 mL of a different concentration of AFP standard antigen for 35 min, followed by washing with doubly distilled water and PBS buffer. Next, the electrode (AuE/GO-Au NPs/Ab1/BSA/AFP) was incubated with 10 μL of Ab2-HRP -Au-PDA-carbon sphere dispersion for 60 min, followed by washing with doubly distilled water and PBS buffer to remove the non-specific adsorption of conjugate. The electrochemical detection was performed in a PBS buffer solution containing 50 μ*M* thionine and 4 m*M* $H_2O_2$. Schematic illustration of the multienzyme labeling amplification strategy using Ab2-HRP-Au-PDA-carbon sphere conjugate is shown in Scheme 3.

## Results and Discussion

**Characterization of GO-Au NPs**

The entire process of self-assembly of GO and Au NPs is shown in Scheme 1. The cationic functional macromolecules of PDDA were adsorbed at the GO, which resulted in positive charges on the surface of GO. Finally, the cationic GO dispersion was directly mixed with the as-prepared solution of Au NPs. Driven by the electrostatic interaction, the citrate-capped Au NPs quickly adhered to the surface of PDDA/GO. The typical SEM images of GO and as-prepared GO-Au NPs hybrids are displayed in Fig. 1. As shown in Fig. 1(a), thin films of oxidizing graphite was observed. After the formation of GO-Au NPs hybrids, it is observed that all the GO nanosheets have been decorated with NPs and nearly all the Au NPs were distributed uniformly at the surface of the GO (Fig. 1(b)), suggesting that the present self-assembly method can effectively produce homogeneous high-loading NPs supported on GO hybrids.


$$H_2O_2 + HRP_{(Red)} \longrightarrow HRP_{(Ox)} + H_2O$$

$$HRP_{(Ox)} + Thionine_{(Red)} \longrightarrow HRP_{(Red)} + Thionine_{(Ox)}$$

$$Thionine_{(Ox)} + 2H^+ + 2e^- \longrightarrow Thionine_{(Red)}$$

Multienzyme labeling amplification strategy using Ab2- HRP –Au-PDA-carbon sphere conjugate

**Scheme 3**

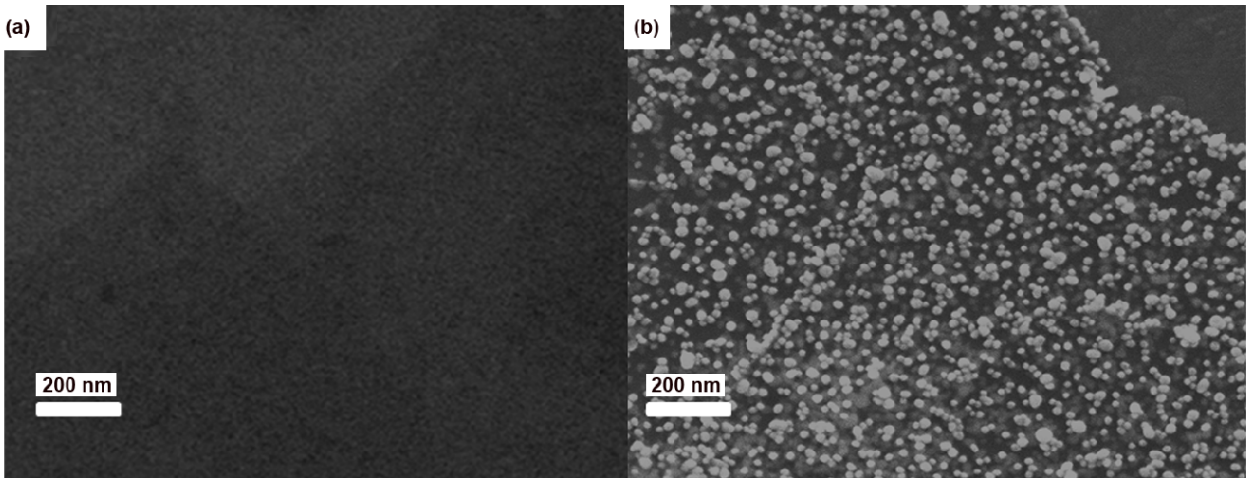


Fig. 1—SEM images of (a) GO and (b) GO-Au NPs hybrids.

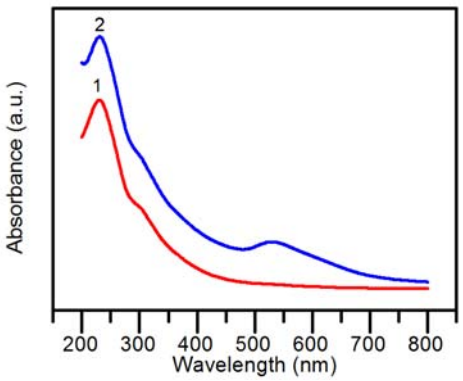


Fig. 2—UV–vis absorption spectra of GO (1), and, GO-Au NPs composites (2) in water.

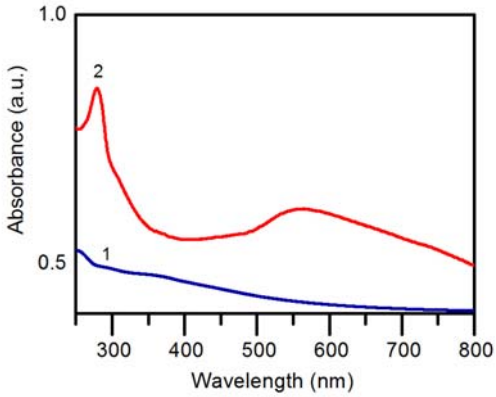


Fig. 3—UV–vis absorption spectra of carbon nanosphere (1), and, Ab2-HRP -Au-PDA-carbon sphere conjugate (2) in water.

UV-vis absorption spectra of the GO and GO-Au NPs hybrids are shown in Fig. 2. Pure GO with two characteristic absorption peaks at 230 and 300 nm originating from π-π* transition of the C=C band and n-π* transition of the C=O band,[30] respectively are observed. Compared with the spectrum of purified GO (Fig. 2, curve 1), a new UV-vis absorption peak of GO-Au NPs hybrids appeared at *ca.* 530 nm (Fig. 2, curve 2), which indicates the capture of AuNPs [31]. The result suggests that some of the surface-modified AuNPs are in close proximity with each other, but were not agglomerated, as evidenced by the SEM images.

UV-vis absorption spectra of the carbon nanospheres and the Ab2-HRP-Au-PDA-carbon sphere Conjugate are shown in Fig 3. Compared with the spectrum of pure colloidal carbon spheres (Fig. 3, curve 1), two new absorption bands centered at 280 nm and 560 nm were observed in the spectrum of the Ab2-HRP-Au-PDA-carbon sphere conjugate (Fig. 3, curve 2). An intense band was observed at 281 nm, which is directly related to the symmetry-forbidden transitions (*La*-*Lb*) of the DA molecule[32]. The absorption bands centered at 560 nm and can be ascribed to the production of AuNPs from the reduction of $HAuCl_4$ by DA in the bionanocomposites. The shift in the resonance wavelength is attributed to interparticle plasmon coupling, a phenomenon observed even when just a few Au NPs or nanorods were clustered together[33]. The result suggests that some of the surface-modified AuNPs were in close proximity with each other but were not agglomerated, as evidenced by the TEM images.

**Signal amplification immunoassay with Ab2-HRP-Au-PDA-carbon sphere conjugate**

To enhance detection sensitivity, herein we pursued a multienzyme labeling strategy instead of a

single-enzyme label during the immunoassay. As shown in Fig. 4, the cyclic voltammogram at AuE/GO-Au NPs /Ab1/BSA/AFP/Ab2-HRP-Au-PDA-carbon sphere electrode (Fig. 4, curve 1) did not show any detectable signal in pH 7.4 PBS. Upon adding 0.05 m*M* thionine to the PBS buffer, the cyclic voltammogram exhibited a pair of stable and well-defined redox peaks (Fig. 4, curve 2), corresponding to the electrochemical oxidation and reduction of thionine. However, after adding 4 m*M* $H_2O_2$ to the PBS buffer, the electrocatalytic current at AuE/GO-AuNPs/Ab1/BSA/AFP/Ab2-HRP-Au-PDA-carbon sphere electrode increased significantly (Fig. 4, curve 3). It is not surprising that the multienzyme-antibody labeling strategy enhanced the detection signal more than the traditionally labeled HRP-Ab2. The achieved amplification of signal is ascribed to the large amount of enzymes loaded on the carbon sphere nanocarrier.

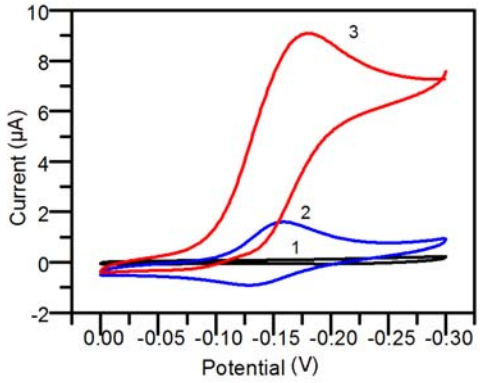


Fig. 4—Cyclic voltammograms obtained at CVs of the AuE/GO-Au NPs/Ab1/BSA/AFP/Ab2-HRP–Au-PDA-carbon sphere electrode in pH 7.4 PBS (curve 1), pH 7.4 PBS containing 0.05 m*M* THI (curve 2), and, pH 7.4 PBS containing 0.05 m*M* THI and 4 m*M* $H_2O_2$ at 50 mV/s (curve 3).

**EIS characterization of the immunosensor**

It is well known that EIS is an excellent technique for investigating the interface properties of surface-modified electrodes. A typical impedance spectrum (presented in the form of the Nyquist plot) exhibits a semicircle near the origin at higher frequencies corresponding to the electron-transfer-limited process and a linear tail at lower frequency range representing the diffusion-limited process. The electron-transfer resistance, $R_{et}$, is the most directive and sensitive parameter that responds to changes on the electrode interface, as represented by the diameter of the semicircle in the Nyquist plot. Figure 5 shows the impedance spectra corresponding to the stepwise modification processes. The bare electrode exhibited an almost straight line that is characteristic of a diffusional limiting step of the electrochemical process (Fig. 5, curve 1). When the electrode was modified with GO-Au NPs, the GO-Au NPs/Au electrode exhibited a small semicircle at high frequencies (Fig. 5, curve 2), i.e., a low resistance on the GO-Au NPs modified electrode, indicating the successful formation of GO-Au NPs film on the electrode surface. After Ab1 molecules were attached to the GO-Au NPs film, a remarkable increase of the semicircle diameter was observed (Fig. 5, curve 3), and a further increase was noticed (Fig. 5, curve 4) when the Ab1/GO-Au NPs /Au electrode was blocked with BSA. The above results clearly confirm that Ab1 and BSA were successfully immobilized on the electrode. The $R_{et}$ increased again after the prepared immunosensor was incubated with AFP solution.

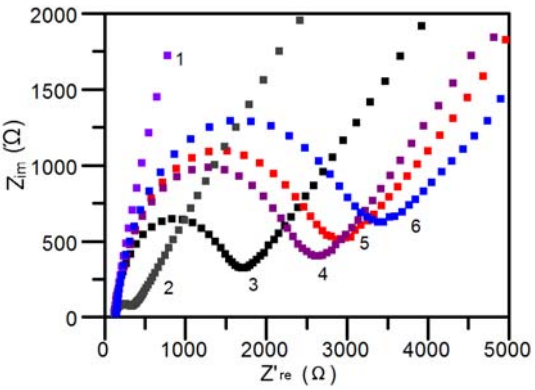


Fig. 5—EIS of the different electrodes. [(1) bare electrode; (2) GO-Au NPs; (3) GO-Au NPs/anti-AFP; (4) GO-Au NPs/anti-AFP/BSA; (5) electrode (4) incubated with 1 ng $mL^{-1}$ AFP; (6) electrode (5) incubated with Ab2-HRP-Au-PDA-carbon sphere in the presence of the redox couple of $Fe(CN)_6^{3-/4-}$ containing 0.10 mol $L^{-1}$ KCl].

When the prepared immunosensor was incubated with HBsAg solution, the formed antigen-antibody immunocomplex formed on the film would further hinder the access of the redox probe to the electrode. Then the resistance increased when Ab2-HRP-Au-PDA-carbon sphere were further incubated with Ab2-HRP-Au-PDA-carbon sphere bioconjugate (Fig. 5, curve 6), which proved that Ab2-HRP-Au-PDA-carbon sphere bioconjugate was also successfully immobilized on the electrode. The EIS change of the modified process indicates that the AuE/GO-Au NPs/Ab1/BSA/AFP/Ab2-HRP-Au-PDA-carbon sphere composite film was successfully formed on electrode surface and suitable for immunosensing.

**Optimization of detection conditions**

The $H_2O_2$ concentration in 5 mL of pH 7.4 PBS buffer on the steady-state current of the immunosensor was studied as it played an important role in the immunosensor performance. When the $H_2O_2$ concentration was less than 4 m*M*, the reduction peak current increased linearly with increasing $H_2O_2$ concentration, and then tended towards a constant value, which corresponded to the saturated station. This shows that the HRP attached to the immunosensor surface had a relatively high catalytic activity. Therefore, the optimal concentration of $H_2O_2$ was chosen at 4 m*M*.

At room temperature, the amperometric responses for AFP increased with the increasing incubation time used in sandwich-type immunoassay and then tended to constant values after 35 min, which showed a saturated binding between the analyte and the capture antibody on electrode surface. Therefore, 35 min of incubation time was selected for the sandwich-type immunoassay.

Due to the co-immobilization of enzymes and antibodies on the carbon sphere nanocarrier, the ratio of HRP and Ab2 (HRP/Ab2) is the most important factor on the response signal. The electrocatalytic current increased with increasing the ratio of HRP/Ab2, and the maximum response was achieved at the ratio of 300:1. The increase of the HRP/Ab2 ratio could increase the total amount of HRP loaded per carbon sphere nanocarrier, which is expected to enhance the response amplification for this sandwich immunoassay. However, the reducing amount of Ab2 in the immunoassay may decrease immunocoupling efficiency to the captured AFP antigen at the electrode surface, which may result in a decreased response. Therefore, the HRP/Ab2 ratio of 300:1 was selected as the optimal condition to prepare the Ab2-HRP-Au-PDA-carbon sphere conjugate.

The effect of the immunochemical incubation temperature (i.e., when the antigen-antibody reaction occurs) was examined at the range from 15-45 °C. It was found that the current response increased with increasing temperature up to 37 °C. The lower response at the incubation temperatures higher than 37 °C may be attributed to an irreversible behavior (denaturation of proteins) involved in the process. Therefore, 37 °C of incubation temperature was selected for the sandwich-type immunoassay.

**Analytical performance**

Under the optimum conditions, the peak currents of the immunosensor array for simultaneous detection of

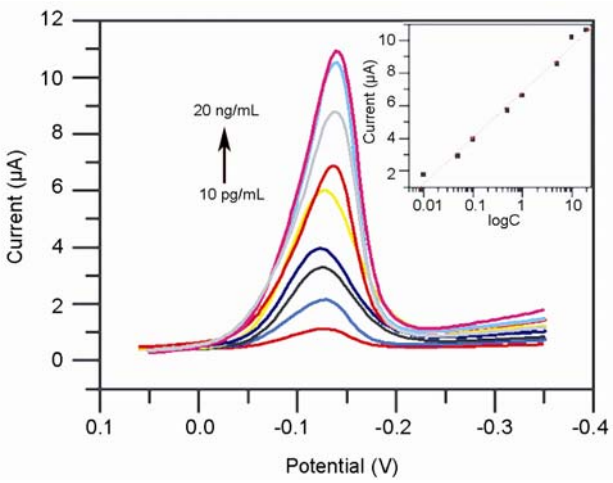


Fig. 6—DPV curves of the immunosensor after incubating with various concentrations of AFP (0, 0.01, 0.05, 0.1, 0.5, 1, 5, 10, and 20 ng $mL^{-1}$ from bottom to top). [Inset: calibration curve of the immonosensor for AFP determination].

AFP increased with the increasing concentration of analytes (Fig. 6). The calibration plots show good linear relationships between the peak currents and the logarithm of the analyte concentrations in the ranges from 10 pg/mL to 20 ng/mL with a correlation coefficient of 0.9942 ($n$ = 6) for AFP. The limits of detection for AFP was 3 pg/mL at a signal-to-noise ratio of 3. The achieved high sensitivity mainly results from the excessive enzymes present in the carbon sphere.

The selectivity of the electrochemical immunoassay was studied using blank PBS and other proteins such as CEA (1 ng/mL), HBsAg (1 ng/mL) and BSA (1 ng/mL). Results clearly show that the sensor response is directly from the binding of AFP to anti-AFP and the level of sensor response depends on the AFP concentration.

## Conclusions

In this work, we have successfully developed a highly sensitive and selective immunosensor for detecting cancer biomarkers and demonstrated this signal amplification procedure. The greatly enhanced sensitivity relies upon two merits: (1) carbon sphere as the enzyme-loading carrier can load many enzyme molecules on each carbon sphere. The labeling protocol allows multiple signals per binding event provided by the use of Ab2-HRP-Au-PDA-carbon sphere instead of conventional HRP-Ab2. (2) GO-Au NPs can provide a high density of primary antibodies because of their high surface area. The resulting

immunosensor possesses high sensitivity, good reproducibility, and cost-effective analytical performance. This method can be expanded for detecting other relevant biomarkers and has the potential for reliable point-of-care diagnostics of cancer and other diseases.

**Acknowledgement**

This work was financially supported by the Open Funds of the State Key Laboratory of Electroanalytical Chemistry(SKLEAC201602) and the Jiangxi Province Food and Drug Administration Science Foundation (2016SP04), China.

**Reference**

1 Wilson G S & Hu Y, *Chem Rev*, 100 (2000) 2693.
2 Warsinke A, Benkert A & Scheller F W, *Fres J Anal Chem*, 366 (2000) 622.
3 Van J M & Lopez-Avila V, *Anal Chem*, 64 (1992) 78A.
4 Bilitewski U, *Anal Chem*, 72 (2000) 692.
5 Gillespie J R & Uversky V N, *Biochim Biophys Acta*, 1480 (2000) 41.
6 Li T X, *In Assay and Clinical Application of AFP*, 1st Edn, (Military Medical Science Press, Beijing) 2001, 169.
7 Matsuya T, Tashiro S, Hoshino N, Shibata N, Nagasaki Y & Kataoka K, *Anal Chem*, 75 (2003) 6124.
8 Wang G L, Yuan J L, Gong B L, Matsumoto K & Hu Z D, *Anal Chim Acta*, 448 (2001) 165.
9 Belanger L, Sylvestre C & Dufour D, *Clin Chim Acta*, 48 (1973) 15.
10 Aguilar Z P, Vandaveer W R & Fritsch I, *Anal Chem*, 74 (2002) 3321.
11 Xu Y Y, Bian C, Chen S F & Xia S H, *Anal Chim Acta*, 561 (2006) 48.
12 Fu Z F, Hao C, Fei X Q & Ju G J, *J Immunol Methods*, 312 (2006) 61.
13 Chen J, Tang J H, Yan F & Ju H X, *Biomaterials*, 27 (2006) 2313.
14 Wang Z J, Yang Y H, Li J S, Gong J L, Shen G L & Yu R Q, *Talanta*, 69 (2006) 686.
15 Liu Y, Wang M K, Zhao F, Xu Z A & Dong S J, *Biosen Bioelect*, 21 (2005) 984.
16 Yang L, Wei W Z, Gao X H, Xia J J & Tao H, *Talanta*, 68 (2005) 40.
17 Mccreery R L, *Chem Rev*, 108 (2008) 2646.
18 Wang H T, Holmberg B A & Yan Y S, *J Mater Chem*, 12 (2002) 3640.
19 Sun X & Li Y, *Angew Chem*, 43 (2004) 597.
20 Feather M S & Harris J F, *Adv Carbo Chem Biochem*, 28 (1973) 161.
21 Shang N G, Papakonstantinou P, McMullan M, Chu M, Stamboulis A, Potenza A, Dhesi S S & Marchetto H, *Adv Func Mater*, 18 (2008) 3506.
22 Tang L H, Wang Y, Li Y M, Feng H B, Lu J & Li J H, *Adv Funct Mater*, 19 (2009) 1.
23 Wang Y, Lu J, Tang L H, Chang H X & Li J H, *Anal Chem*, 81 (2009) 9710.
24 Kang X H, Wang J, Kang X H, Wu H, Aksay I A, Liu J & Lin Y Hm, *Biosen Bioelect*, 25 (2009) 901.
25 Zhou M, Zhai Y M & Dong S J, *Anal Chem*, 81 (2009) 5603.
26 Alwarappan S, Erdem A, Liu C & Li C Z, *J Phys Chem C*, 113 (2009) 8853.
27 Wang Y, Wei H, Li B, Ren W, Guo S, Dong S & Wang E, *Chem Comm*, 48 (2007) 5220.
28 Hummers W S & Offeman R E, *J Am Chem Soc*, 80 (1958) 1339.
29 Shin Y, Wang L Q & Bae I T, *J Phys Chem C*, 112 (2008) 14236.
30 Chen J L, Yan X P, Meng K & Wang S F, *Anal Chem*, 83 (2011) 8787.
31 Cui R, Liu C, Shen J, Gao D, Zhu J J & Chen H Y, *Adv Func Mater*, 18 (2008) 2197.
32 Tan Y, Deng W, Li Y, Huang Z, Meng Y, Xie Q, Ma M & Yao S, *J Phys Chem B*, 114 (2010) 5016.
33 Fu Y C, Xie Q J, Jia X E, Xu X H, Meng W H & Yao S Z, *J Electroanal Chem*, 603 (2007) 96.